

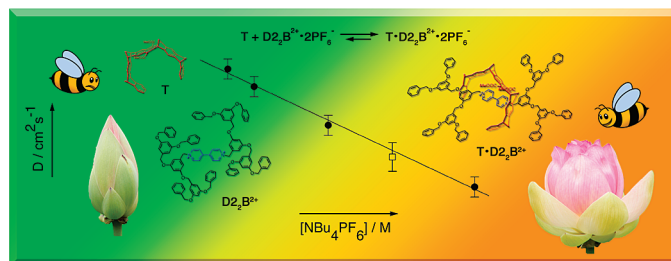
## Tweezering the Core of Dendrimers: Medium Effect on the Kinetic and Thermodynamic Properties

Carlo Giansante,<sup>†</sup> Andrea Mazzanti,<sup>‡</sup> Massimo Baroncini,<sup>†</sup> Paola Ceroni,<sup>\*,†</sup> Margherita Venturi,<sup>†</sup> Frank-Gerrit Klärner,<sup>§</sup> and Fritz Vögtle<sup>⊥</sup>

<sup>†</sup>Dipartimento di Chimica "G. Ciamician", Alma Mater Studiorum, Università di Bologna, Via Selmi 2, 40126 Bologna, Italy, <sup>‡</sup>Dipartimento di Chimica Organica "A. Mangini", Alma Mater Studiorum, Università di Bologna, Viale Risorgimento 4, 40136 Bologna, Italy, <sup>§</sup>Institut für Organische Chemie der Universität Essen–Duisburg, Campus Essen Universitätsstrasse 5, D-45117 Essen, Germany, and <sup>⊥</sup>Kekulé-Institut für Organische Chemie und Biochemie der Universität Bonn, Gerhard-Domagk Strasse 1, D-53121 Bonn, Germany

paola.ceroni@unibo.it

Received July 3, 2009



We have investigated the complex formation between dendritic guests and a molecular tweezer host by NMR, absorption, and emission spectroscopy as well as electrochemical techniques. The dendrimers are constituted by an electron-acceptor 4,4'-bipyridinium core appended with one ( $D_nB^{2+}$ ) or two ( $D_{n2}B^{2+}$ ) polyaryl-ether dendrons. Tweezer **T** comprises a naphthalene and four benzene components bridged by four methylene groups. Medium effects on molecular recognition phenomena are discussed and provide insight into the conformation of dendrimers: change in solvent polarity from pure  $CH_2Cl_2$  to  $CH_2Cl_2/CH_3CN$  mixtures and addition of tetrabutylammonium hexafluorophosphate ( $NBu_4PF_6$ , up to 0.15 M), the supporting electrolyte used in the electrochemical measurements, have been investigated. The association constants measured in different media show the following trend: (i) they decrease upon increasing polarity of the solvent, as expected for host–guest complexes stabilized by electron donor–acceptor interactions; (ii) no effect of generation and number of dendrons (one for the  $D_nB^{2+}$  family and two for the  $D_{n2}B^{2+}$  family) appended to the core is observed in higher polarity media; and (iii) in a low-polarity solvent, like  $CH_2Cl_2$ , the stability of the inclusion complexes is higher for  $D_nB^{2+}$  dendrimers than for  $D_{n2}B^{2+}$  ones, while within each dendrimer family it increases by decreasing dendron generation, and upon addition of  $NBu_4PF_6$ . The last result has been ascribed to a partial dendron unfolding. Kinetic investigations performed in lower polarity media evidence that the rate constants of complex formation are slower for symmetric  $D_{n2}B^{2+}$  dendrimers than for the nonsymmetric  $D_nB^{2+}$  ones, and that within the  $D_{n2}B^{2+}$  family, they decrease by increasing dendron generation. The dependence of the rate constants for the formation and dissociation of the complexes upon addition of  $NBu_4PF_6$  has also been investigated and discussed.

### Introduction

Molecular recognition is defined by the information and the energy involved in selection and binding of substrate(s) by a given receptor molecule.<sup>1</sup> Molecular recognition phe-

nomena imply the formation of supramolecular species characterized by peculiar structural, thermodynamic, and

(1) Lehn, J. M. *Supramolecular Chemistry: Concepts and Perspectives*; VCH: Weinheim, Germany, 1995.

kinetic features determined by molecular information stored in receptor and substrate(s) that lead to selective binding. Stability of the supramolecular host–guest complex substantially depends on the medium and results from a subtle balance between solvation<sup>2</sup> (of both receptor and substrate) and complexation (i.e., “solvation” of the substrate by the receptor).<sup>1</sup>

Dendrimers<sup>3</sup> are repeatedly branched molecules that can contain selected functional groups in predetermined sites of their multiarmed structure. In spite of their large structures, that usually make dendrimers attractive as host molecules, suitably designed dendrimers can be involved as guests in molecular recognition phenomena.<sup>4</sup> In such cases, the host species does not interact with the whole dendritic structure, but only with specific component units. In particular, we have previously reported<sup>5</sup> that dendrimers containing an electron-acceptor 4,4'-bipyridinium core<sup>6</sup> appended with one ( $D_nB^{2+}$ ) or two ( $D_{n_2}B^{2+}$ ) polyaryl-ether dendrons (Scheme 1) are known to function as guests in molecular recognition phenomena involving a concave electron-donor molecule comprising a naphthalene and four benzene components bridged by four methylene groups<sup>7</sup> (tweezer **T** in Scheme 1). The  $D_{n_m}B^{2+}$  dendrimers show an amphiphilic character since they are constituted of a hydrophilic 4,4'-bipyridinium core surrounded by hydrophobic 1,3-dimethyleneoxybenzene-based dendrons. Therefore, the medium may affect the shape of the dendrimers.

Here we examine the effects induced by a change in solvent polarity and addition of tetrabutylammonium hexafluorophosphate, hereafter indicated as  $NBu_4PF_6$ , on the thermodynamic and kinetic features of the host–guest complex formation between the  $D_{n_m}B^{2+}$  substrates and the endoreceptor tweezer **T**. Characterization of host–guest complexes based on charge-transfer interactions often combines spectroscopic and electrochemical studies, but conventional electrochemical techniques require the presence of supporting electrolytes that may affect the stability and the kinetics of

complex formation, especially if host and/or guest are charged species. In this regard, it has been shown that redox processes in nonaqueous solutions may be very sensitive to changes in solvents and supporting electrolytes.<sup>8</sup> Furthermore, the presence of salts has been demonstrated to affect electron-transfer processes in supramolecular adducts formed by donor/acceptor interactions.<sup>9,10</sup>

## Results and Discussion

**Photophysical and Electrochemical Properties of Tweezer T.** In  $CH_2Cl_2$  solution, **T** shows relatively weak, low-energy absorption bands, and a strong fluorescence band ( $\lambda_{max} = 344$  nm,  $\tau = 9.5$  ns,  $\Phi = 0.53$ ) typical of the naphthalene chromophoric group. In  $CH_2Cl_2/CH_3CN$  9:1 (v/v) solution, **T** shows an irreversible oxidative process at +1.6 V, whereas no reduction process has been observed in the potential window of the solvent used (up to –2.0 V vs. SCE).

**Photophysical and Electrochemical Properties of Dendrimers  $D_{n_m}B^{2+}$ .** The investigated dendrimers contain three types of chromophoric groups, namely a 4,4'-bipyridinium unit at the core, 1,3-dimethyleneoxybenzene units in the branches, and benzene units at the periphery. Dendrimers exhibit a strong absorption band in the UV region that does not coincide with the summation of the spectra of the component units, particularly because of the presence of a broad and weak absorption tail at  $\lambda > 300$  nm that is assigned to a charge-transfer transition from 1,3-dimethyleneoxybenzene electron-donor units to the 4,4'-bipyridinium electron-acceptor core. Dimethyleneoxybenzene and, accordingly, Fréchet-type dendrons<sup>11</sup> are known to exhibit fluorescence ( $\lambda_{max} = 350$  nm and  $\tau < 1$  ns). Dendrimers, instead, are not fluorescent because the excited state localized on the 1,3-dimethyleneoxybenzene units is deactivated via a fast electron-transfer process to the 4,4'-bipyridinium, as revealed by transient absorption measurements.<sup>12</sup> The 4,4'-bipyridinium core,  $B^{2+}$ , is a well-known electroactive unit that undergoes two successive, reversible, one-electron reduction processes at easily accessible potentials that correspond to the formation of a radical cation ( $B^{2+} \rightarrow B^{\cdot+}$ ) and a neutral ( $B^{\cdot+} \rightarrow B$ ) species.<sup>5</sup> In agreement with these expectations, the  $D_{n_m}B^{2+}$  nonsymmetric dendrimers, as well as the  $D_{n_2}B^{2+}$  symmetric ones show two reversible one-electron transfer processes. The half-wave potential values ( $E_{1/2}$ ) observed for reduction of the six dendrimers, gathered in Table 1, show that the 4,4'-bipyridinium electrochemical behavior is slightly affected by the presence of the dendritic branches: (i) the reduction potentials are slightly shifted toward negative potentials (30–40 mV) for the nonsymmetric dendrimers compared to the symmetric ones and (ii), within each family, the first generation dendrimer shows a slight negative shift of the potentials for both the reduction processes compared to the second and third generation dendrimers. The heterogeneous

(2) Reichardt, C. *Solvents and Solvent Effects in Chemistry*; 3rd ed.; Wiley-VCH: Weinheim, Germany, 2003.

(3) (a) Newkome, G. R.; Moorefield, C.; Vögtle, F. *Dendrimers and Dendrons: Concepts, Syntheses, Perspectives*; Wiley-VCH: Weinheim, Germany, 2001. (b) *Dendrimers and other Dendritic Polymers*; Fréchet, J. M. J., Tomalia, D. A., Eds.; Wiley: New York, 2001. (c) Vögtle, F.; Richardt, G.; Werner, N. *Dendrimer Chemistry*; Wiley-VCH: Weinheim, Germany, 2009.

(4) For some recent examples, see: (a) Ong, W.; Gómez-Kaifer, M.; Kaifer, A. E. *Chem. Commun.* **2004**, 1677. (b) Sobransingh, D.; Kaifer, A. E. *Chem. Commun.* **2005**, 5071. (c) Ong, W.; Grindstaff, J.; Sobransingh, D.; Toba, R.; Quintela, J. M.; Peinador, C.; Kaifer, A. E. *J. Am. Chem. Soc.* **2005**, *127*, 3353. (d) Bruinink, C. M.; Nijhuis, C. A.; Peter, M.; Dordi, B.; Crespo-Biel, O.; Auletta, T.; Mulder, A.; Schoenherr, H.; Vancso, G. J.; Huskens, J.; Reinhoudt, D. N. *Chem.—Eur. J.* **2005**, *11*, 3988. (e) Wang, W.; Kaifer, A. E. *Angew. Chem., Int. Ed.* **2006**, *45*, 7042. (f) Ornelas, C.; Ruiz Aranzaes, J.; Cloutet, E.; Alves, S.; Astruc, D. *Angew. Chem., Int. Ed.* **2007**, *46*, 872. (g) Hahn, U.; Cardinali, F.; Nierengarten, J. F. *New J. Chem.* **2007**, *31*, 1128. (h) Branchi, B.; Ceroni, P.; Balzani, V.; Bergamini, G.; Klärner, F.-G.; Vögtle, F. *Chem.—Eur. J.* **2009**, *15*, 7876.

(5) (a) Balzani, V.; Ceroni, P.; Giansante, C.; Vicinelli, V.; Klärner, F.-G.; Verhaelen, C.; Vögtle, F.; Hahn, U. *Angew. Chem., Int. Ed.* **2005**, *44*, 4574. (b) Balzani, V.; Bandmann, H.; Ceroni, P.; Giansante, C.; Hahn, U.; Klärner, F.-G.; Müller, W. M.; Müller, U.; Verhaelen, C.; Vicinelli, V.; Vögtle, F. *J. Am. Chem. Soc.* **2006**, *128*, 637.

(6) (a) Monk, P. M. S. *The Viologens: Physicochemical Properties, Synthesis, and Applications of the Salts of 4,4'-Bipyridine*; Wiley: New York, 1998. (b) Ballardini, R.; Credi, A.; Gandolfi, M. T.; Giansante, C.; Marconi, G.; Silvi, S.; Venturi, M. *Inorg. Chim. Acta* **2007**, *360*, 1072.

(7) (a) Klärner, F.-G.; Burkert, U.; Kamieth, M.; Boese, M. *J. Phys. Org. Chem.* **2000**, *13*, 604. (b) Klärner, F.-G.; Kahlert, B. *Acc. Chem. Res.* **2003**, *36*, 919. (c) Marchioni, F.; Juris, A.; Lobert, M.; Seelbach, U. P.; Kahlert, B.; Klärner, F.-G. *New J. Chem.* **2005**, *29*, 780.

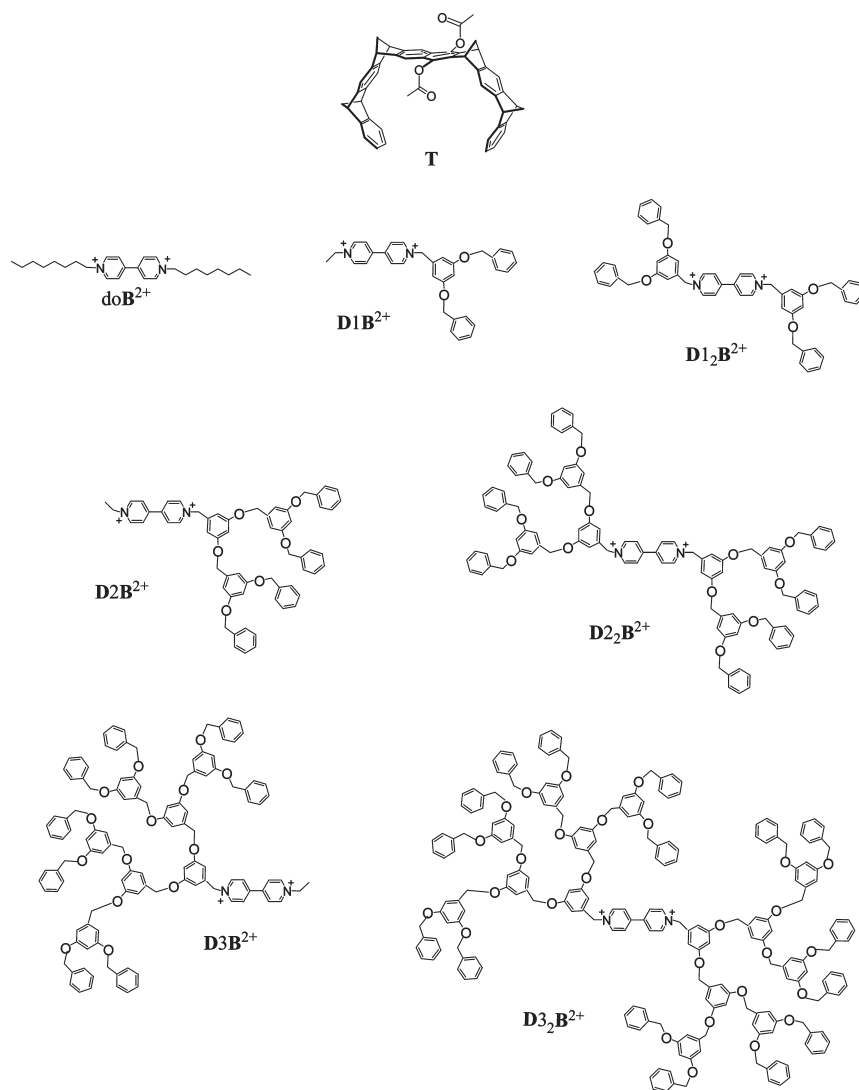
(8) Barriere, F.; Geiger, W. E. *J. Am. Chem. Soc.* **2006**, *128*, 3980.

(9) Ion–radical pairs are formed upon photoinduced electron transfer of the corresponding ground state charge-transfer complex: (a) Thompson, P. A.; Simon, J. D. *J. Am. Chem. Soc.* **1993**, *115*, 5657. (b) Masnovi, J. M.; Levine, A.; Kochi, J. K. *J. Am. Chem. Soc.* **1985**, *107*, 4365.

(10) Both charge- and electron-transfer processes occur at the ground state: Rosokha, S. V.; Sun, D.; Fisher, J.; Kochi, J. K. *ChemPhysChem.* **2008**, *9*, 2406.

(11) Stewart, G. M.; Fox, M. A. *J. Am. Chem. Soc.* **1996**, *118*, 4354.

(12) Ceroni, P.; Giansante, C.; Maestri, M.; Vicinelli, V. Unpublished results.

SCHEME 1. Formulas of the Investigated Compounds and Abbreviations Used<sup>a</sup>

<sup>a</sup>The tweezer-shaped host is T; the dendrimers are generically indicated as  $D_n m B^{2+}$ , where  $B^{2+}$  stands for the 4,4'-bipyridinium core and D for the 1,3-dimethyleneoxybenzene-based dendrons;  $n$  indicates the dendron generation ( $n = 1, 2, 3$ ) and  $m$  the number of dendrons attached to the core:  $m = 1$  stands for nonsymmetric  $D_n B^{2+}$  dendrimers, while  $m = 2$  for the symmetric  $D_n 2B^{2+}$  ones. Hexafluorophosphate counteranions have been omitted for clarity.

TABLE 1. Half-Wave Potentials (V vs. SCE) in  $CH_2Cl_2/CH_3CN$  9:1 (v/v),  $NBu_4PF_6$  0.1 M, Except as Otherwise Noted

	$B^{2+} \rightarrow B^{\cdot+}$	$B^{\cdot+} \rightarrow B$
$D1B^{2+}$	-0.29	-0.77
$D2B^{2+}$	-0.27	-0.73
$D3B^{2+}$	-0.27	-0.73
$D1_2B^{2+}$ <sup>a</sup>	-0.25	-0.73
$D2_2B^{2+}$	-0.24	-0.72
$D3_2B^{2+}$	-0.24	-0.72

<sup>a</sup> $CH_2Cl_2/CH_3CN$  3:1 (v/v).

rate of electron transfer to the electrode surface is high for all the dendrimers. For example, in the case of  $(D3)_2B^{2+}$  the two reduction processes show a Nernstian behavior at scan rates up to 5 V/s, thereby indicating no significant inhibition or site isolation effect on the dendrimer core by the dendrons.

**<sup>1</sup>H NMR Spectra of Dendrimers in Different Media.** As an example the case of the symmetric second generation dendrimer is discussed in detail. <sup>1</sup>H NMR spectra of 0.4 mM

$D2_2B^{2+}$  recorded in  $CD_3CN$  (Figure 1c) or  $CD_3COCD_3$ <sup>13</sup> at 295 K are characterized by sharp and well-resolved resonances.

On the other hand, the <sup>1</sup>H NMR spectrum of 0.4 mM  $D2_2B^{2+}$  in  $CD_2Cl_2/CD_3CN$  9:1 (v/v) at 295 K (Figure 1a) shows broad resonances for inner protons of the 4,4'-bipyridinium core, while aromatic protons at the periphery of the dendrons are well resolved.<sup>14</sup> This behavior can be explained by many different processes, such as change in dendrimer conformation (dendron folding/unfolding), formation of aggregates,<sup>13</sup> and ion pairing with  $PF_6^-$  counterions. The last hypothesis can be ruled out since, on the basis of the results obtained in the association with the tweezer (see

(13) Ceroni, P.; Vicinelli, V.; Maestri, M.; Balzani, V.; Müller, W. M.; Müller, U.; Hahn, U.; Osswald, F.; Vögtle, F. *New J. Chem.* **2001**, 25, 989.

(14) The line broadening of the signals belonging to the bipyridyl core is mainly due to a very short longitudinal relaxation time  $T_1$ . This finding may reflect the different solvation of the core in the two different solvents, i.e.,  $CD_2Cl_2$  and  $CD_3CN$ .

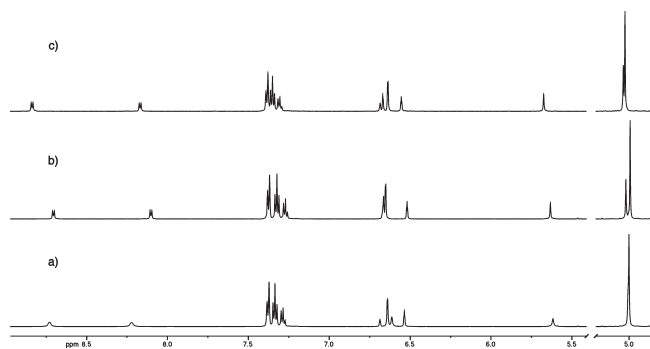


**FIGURE 1.**  $^1\text{H}$  NMR spectra (600 MHz) at 295 K of  $\text{D}_2\text{B}^{2+}$  0.4 mM in (a)  $\text{CD}_2\text{Cl}_2/\text{CD}_3\text{CN}$  9:1 (v/v), (b)  $\text{CD}_2\text{Cl}_2/\text{CD}_3\text{CN}$  9:1 (v/v) and 0.15 M  $\text{NBu}_4\text{PF}_6$ , and (c)  $\text{CD}_3\text{CN}$ .

below), the bipyridinium core and the  $\text{PF}_6^-$  counterions form a tight ion pair. To discriminate between *intradendrimer* (dendron folding/unfolding) and *interdendrimer* (e.g., formation of aggregates between bipyridinium cores<sup>15</sup> of different dendrimers) processes, NMR spectra of  $\text{D}_2\text{B}^{2+}$  at different concentrations have been recorded in  $\text{CD}_2\text{Cl}_2/\text{CD}_3\text{CN}$  9:1 (v/v) solution at 295 K: no change has been observed at concentrations ranging between  $1 \times 10^{-4}$  and  $5 \times 10^{-3}$  M. It follows that formation of aggregates is unlikely to occur, especially in the dilute solutions ( $\approx 10^{-5}$  M) used for fluorescence measurements. Indeed, normalized UV–vis absorption spectra of an air-equilibrated  $\text{CH}_2\text{Cl}_2/\text{CH}_3\text{CN}$  9:1 (v/v) solution of  $\text{D}_2\text{B}^{2+}$  at 298 K coincide in the  $1 \times 10^{-6}$  to  $5 \times 10^{-4}$  M concentration range.

These findings rule out interdendrimer processes and point to a change in dendrimer conformation. In particular, a folding of dendrons around the dendritic core is likely to occur in low-polarity solvent, as confirmed by other measurements (see below).

To obtain more insight on this conformational change we performed  $^1\text{H}$  NMR measurements in the presence of increasing quantity of  $\text{NBu}_4\text{PF}_6$  aimed at reproducing the electrochemical conditions. Indeed, under such conditions,  $\text{CH}_2\text{Cl}_2/\text{CH}_3\text{CN}$  9:1 (v/v) with 0.1 M  $\text{NBu}_4\text{PF}_6$  as supporting electrolyte, no significant inhibition or site isolation effect on the dendrimer core by the dendrons has been evidenced.<sup>5</sup>

Titration of a  $\text{CD}_2\text{Cl}_2/\text{CD}_3\text{CN}$  9:1 (v/v) solution containing 0.4 mM  $\text{D}_2\text{B}^{2+}$  with  $\text{NBu}_4\text{PF}_6$  results in a gradual sharpening (see, e.g., Figure 1b) of the resonances of the  $^1\text{H}$  NMR spectra with peak shapes resembling those obtained in  $\text{CD}_3\text{CN}$ . In addition,  $^1\text{H}$  NMR spectra of 0.4 mM  $\text{D}_2\text{B}^{2+}$  in  $\text{CD}_3\text{CN}$  solution have been found almost insensitive to  $\text{NBu}_4\text{PF}_6$  addition. These results clearly indicate that the  $\text{NBu}_4\text{PF}_6$  salt cannot be considered inert. In low-polarity solvent it affects the environment that becomes similar to that experienced by the dendrimers in high-polarity solvents. As a consequence the dendrimer conformation

(15) A somehow related molecule consisting of three arms each containing 4,4'-bipyridinium units attached covalently to a 1,3,5-trisubstituted benzene central core and each bearing at its other end a bulky hydrophobic tetraarylmethane-based terminating group revealed, in chloroform solution, the formation of aggregates, see: Amabilino, D. B.; Asakawa, M.; Ashton, P. R.; Ballardini, R.; Balzani, V.; Belohradsky, M.; Credi, A.; Higuchi, M.; Raymo, F. M.; Shimizu, T.; Stoddart, J. F.; Venturi, M.; Yase, K. *New J. Chem.* **1998**, 22, 959.

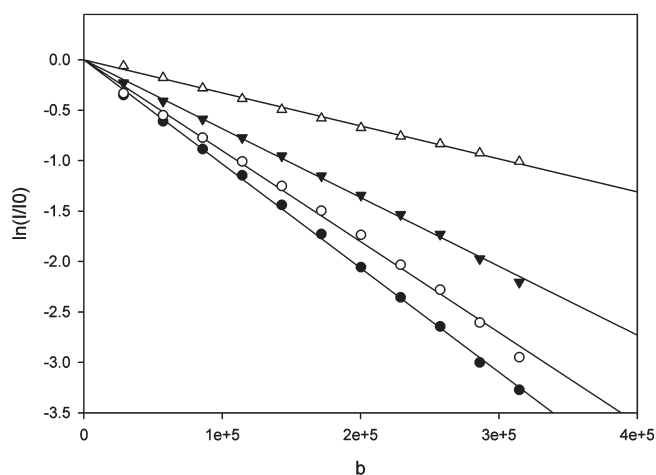


**FIGURE 2.** Stejskal–Tanner plots of a  $\text{CD}_2\text{Cl}_2/\text{CD}_3\text{CN}$  9:1 (v/v) solution containing 0.4 mM  $\text{D}_2\text{B}^{2+}$  at 295 K in the presence of increasing amounts of  $\text{NBu}_4\text{PF}_6$ : 0 (solid circles), 15 (open circles), 60 (solid triangles), and 150 mM (open triangles).

changes, most probably leading to unfolding of the dendritic structure.

**Diffusion Coefficients of Dendrimers Measured by NMR Experiments.** Pulse gradient stimulated echo NMR techniques<sup>16</sup> have been used to gain information on the conformation of the dendrimers through their diffusion in different media. In the present case, DOSY experiments<sup>17</sup> have been performed on a  $\text{CD}_2\text{Cl}_2/\text{CD}_3\text{CN}$  9:1 (v/v) solution containing 0.4 mM  $\text{D}_2\text{B}^{2+}$  in the presence of increasing amounts of  $\text{NBu}_4\text{PF}_6$  up to 0.15 M.

Decays of the signal corresponding to the  $\text{Ar}-\text{CH}_2\text{O}$  protons at 5 ppm as a function of the pulsed gradient strength have been plotted (Figure 2) according to the Stejskal–Tanner eq 1:<sup>18</sup>

$$\ln \frac{I}{I_0} = -\delta^2 \gamma^2 G^2 (\Delta - \delta/3) D \quad (1)$$

where  $\gamma$  is the gyromagnetic ratio,  $\delta$  is the duration of the pulse,  $G$  is the pulsed gradient strength,  $\Delta$  is the time separation between the pulsed gradients, and  $D$  is the diffusion coefficient. The product  $\delta^2 \gamma^2 G^2 (\Delta - \delta/3)$  is termed the  $b$  value. The plot of  $\ln(I/I_0)$  versus the  $b$  values for an isotropic solution gives a straight line, with a slope of  $-D$ .

In the case of the examined dendrimer (Figure 2), Stejskal–Tanner plots are linear both in the absence and in the presence of  $\text{NBu}_4\text{PF}_6$  and reveal that the diffusion coefficient of  $\text{D}_2\text{B}^{2+}$  decreases linearly with increasing salt concentration (Figure 3): a more than 3-fold decrease is observed on going from 0 to 0.15 M  $\text{NBu}_4\text{PF}_6$ .

The diffusion coefficient  $D$  can be related to the hydrodynamic radius  $r_h$  by the Stokes–Einstein equation, derived by assuming that a spherical particle of colloidal dimension moves with uniform velocity in a fluid continuum. For compounds having a van der Waals volume much bigger than the volume of the solvent molecules, “sticking” boundary conditions are applicable, and the nonspherical form of the molecule has little influence since it moves together with

(16) Cohen, Y.; Avram, L.; Frish, L. *Angew. Chem., Int. Ed.* **2005**, 44, 520.

(17) Johnson, C. S., Jr. *Prog. Nucl. Magn. Reson. Spectrosc.* **1999**, 34, 203.

(18) Stejskal, O. E.; Tanner, J. E. *J. Chem. Phys.* **1965**, 42, 288.

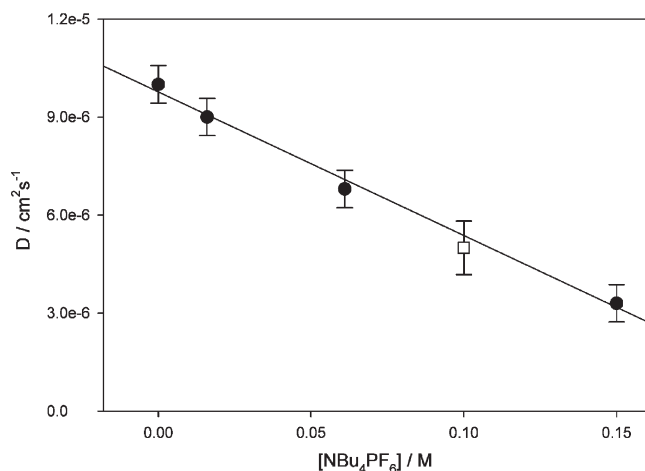


**FIGURE 3.** Diffusion coefficient values of 0.4 mM  $\text{D}_{22}\text{B}^{2+}$  in air-equilibrated  $\text{CD}_2\text{Cl}_2/\text{CD}_3\text{CN}$  9:1 (v/v) solution determined by DOSY experiments as a function of  $\text{NBu}_4\text{PF}_6$  concentration (solid circles). Open square represents the diffusion coefficient value of  $\text{D}_{22}\text{B}^{2+}$  in argon-purged  $\text{CH}_2\text{Cl}_2/\text{CH}_3\text{CN}$  9:1 (v/v) solution containing 0.1 M  $\text{NBu}_4\text{PF}_6$ , obtained by chronoamperometric experiments.

solvent molecules.<sup>19</sup> Under these assumptions, the diffusion coefficient  $D$  is inversely proportional to the hydrodynamic radius,  $r_h$ , and the medium viscosity  $\eta$ , according to eq 2:

$$r_h = (kT)/(6\pi\eta D) \quad (2)$$

where  $k$  is the Boltzmann constant and  $T$  is the temperature.

By taking into account the medium viscosity that changes from 0.6759 mPa·s for a  $\text{CH}_2\text{Cl}_2/\text{CH}_3\text{CN}$  9:1 (v/v) mixture to 0.8060 mPa·s for the same solvent mixture in the presence of 0.15 M  $\text{NBu}_4\text{PF}_6$ , the hydrodynamic radius of the dendrimer increases by a factor of 2.5. This value is quite large and can be partly due to the fact that the assumptions leading to eq 2 are not fully applicable to the present case.

Because the aggregate formation can be ruled out (vide supra), the observed trend has to be mainly attributed to an increase in dendrimer volume upon unfolding of the dendrons.

Steady-state cyclic voltammetric and chronoamperometric measurements with ultramicroelectrodes<sup>20</sup> provides an independent measure of diffusion coefficient for  $\text{D}_{22}\text{B}^{2+}$  in  $\text{CH}_2\text{Cl}_2/\text{CH}_3\text{CN}$  9:1 (v/v) in the presence of 0.1 M  $\text{NBu}_4\text{PF}_6$  (open square in Figure 3). Such a value is interpolated by the linear regression of the diffusion coefficients of  $\text{D}_{22}\text{B}^{2+}$  in  $\text{CD}_2\text{Cl}_2/\text{CD}_3\text{CN}$  9:1 (v/v) at different salt concentrations determined by using the DOSY technique (Figure 3). The necessity to take into account the effect of supporting electrolyte addition in measuring diffusion coefficients has already been stressed by Kaifer et al.<sup>21</sup>

#### Thermodynamics of Host–Guest Complex Formation.

**(1) Electrochemical Measurements.** Host–guest complex formation between tweezer **T** and  $\text{D}_n\text{B}^{2+}$  dendrimers is essentially driven by electron-donor/acceptor interactions between the electron-acceptor core of the dendrimers and

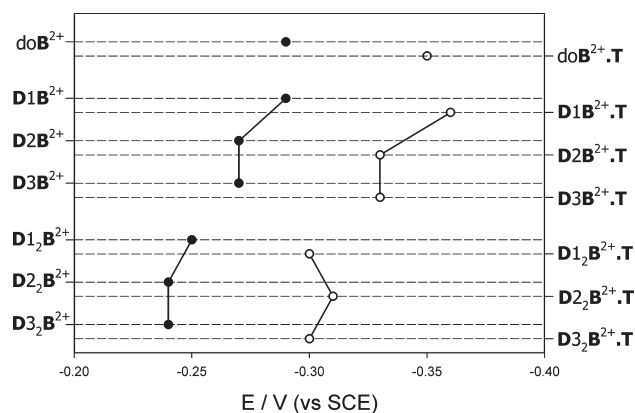


**FIGURE 4.** Half-wave potentials for the first reduction processes of  $\text{doB}^{2+}$  model compound and  $\text{D}_n\text{B}^{2+}$  dendrimers (filled circles), and of their host–guest complexes with tweezer **T** (open circles) in argon-purged  $\text{CH}_2\text{Cl}_2/\text{CH}_3\text{CN}$  9:1 (v/v) containing 0.1 M  $\text{NBu}_4\text{PF}_6$ . Under the experimental conditions used, more than 95% of the electroactive species is engaged in the complex formation. For solubility problems the  $\text{D}_{12}\text{B}^{2+}$  dendrimer and the  $\text{D}_{12}\text{B}^{2+}\cdot\text{T}$  complex have been studied in argon-purged  $\text{CH}_2\text{Cl}_2/\text{CH}_3\text{CN}$  3:1 (v/v) solution containing 0.1 M  $\text{NBu}_4\text{PF}_6$ .

the electron-donor cavity of the host. Clear evidence of the complex formation is given by the half-wave potential values ( $E_{1/2}$ ), corresponding to the first one-electron reduction process of the 4,4'-bipyridinium dendritic cores that move toward more negative values upon host addition (compare open and filled circles of Figure 4) because the electron-withdrawing character of the dendritic cores is reduced by the interaction with the electron-donor cavity of **T**.

Both geometrical and interactional complementarity requirements are fulfilled in the formation of these host–guest complexes. Upon one-electron reduction of the 4,4'-bipyridinium dendritic core, however, the interactional complementarity between receptor **T** and monoreduced  $\text{D}_n\text{B}^{\cdot+}$  species is weakened. Thereby dissociation of the inclusion complexes occurs as demonstrated by the fact that the second reduction process of the bipyridinium core takes place at the same potential value in the absence and in the presence of **T**.<sup>5</sup>

**(2) Photophysical Measurements.** Titrations of  $\text{CH}_2\text{Cl}_2$  air-equilibrated solutions of **T** (ca. 15  $\mu\text{M}$ ) with solutions of  $\text{D}_n\text{B}^{2+}$  dendrimers and  $\text{doB}^{2+}$  model compound evidence a strong decrease of the **T** emission band. As an example, in Figure 5 the data obtained for  $\text{D}_{32}\text{B}^{2+}$  are reported (black lines). Time-resolved fluorescence measurements support a static quenching mechanism due to host–guest complex formation; the fluorescence lifetime of **T** is, indeed, not affected upon dendrimer addition, and there is no evidence of a double exponential decay. Therefore, the observed fluorescence intensity can be assigned to the uncomplexed host molecules.<sup>5</sup>

Fitting of the experimental fluorescence intensities (see the Experimental Section) is fully satisfactory ( $r^2 > 0.99$  for the data shown in the inset of Figure 5). The corresponding association constants (Table 2) are of the order of  $10^4 \text{ M}^{-1}$  in  $\text{CH}_2\text{Cl}_2$  solution and a comparison of the obtained values evidences that (i) the complexes involving nonsymmetric  $\text{D}_n\text{B}^{2+}$  dendrimers are more stable than those formed by the symmetric  $\text{D}_n\text{B}^{2+}$  analogues and (ii) upon increasing dendrimer generation, the stability of the complexes decreases

(19) Macchioni, A.; Ciancaleoni, G.; Zuccaccia, C.; Zuccaccia, D. *Chem. Soc. Rev.* **2008**, *37*, 479.

(20) Denuault, G.; Mirkin, M. V.; Bard, A. J. *J. Electroanal. Chem.* **1991**, *308*, 27.

(21) Sun, H.; Chen, W.; Kaifer, A. E. *Organometallics* **2006**, *25*, 1828.

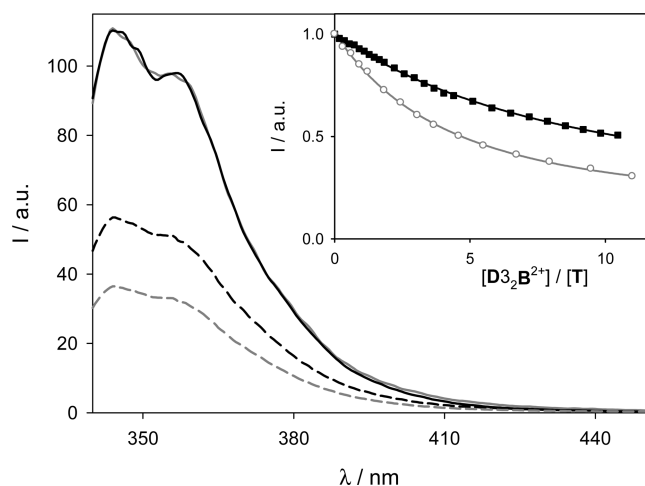


**FIGURE 5.** Fluorescence spectra of a 16  $\mu\text{M}$  air-equilibrated  $\text{CH}_2\text{Cl}_2$  solution of **T** upon addition of 0 (solid lines) and 10 equiv (dashed lines) of  $\text{D}_3\text{B}^{2+}$  in the absence (black lines) and presence (gray lines) of 0.14 M  $\text{NBu}_4\text{PF}_6$ ;  $\lambda_{\text{exc}} = 334$  nm, 298 K. The inset shows the corrected emission intensities of **T** at 356 nm as a function of the added equivalents of  $\text{D}_3\text{B}^{2+}$ , in the absence (black squares) and presence (gray open circles) of 0.14 M  $\text{NBu}_4\text{PF}_6$ . The solid lines show the corresponding fitting based on the formation of a 1:1 complex.

**TABLE 2.** Association Constants for Complexes between host **T** and  $\text{D}_n\text{B}^{2+}$  Dendritic Guests or  $\text{doB}^{2+}$  Model Compound in Air-Equilibrated  $\text{CH}_2\text{Cl}_2$  and  $\text{CH}_2\text{Cl}_2/\text{CH}_3\text{CN}$  1:3 (v/v) Solution at 298 K

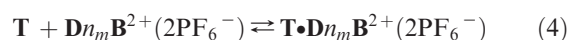
	$K_{\text{ass}}/10^3 \text{ M}^{-1}$	
	$\text{CH}_2\text{Cl}_2$	$\text{CH}_2\text{Cl}_2/\text{CH}_3\text{CN}$ 1:3 (v/v)
$\text{doB}^{2+}$	23	1.9
$\text{D1B}^{2+}$	34	2.4
$\text{D2B}^{2+}$	22	2.9
$\text{D3B}^{2+}$	16	2.2
$\text{D1}_2\text{B}^{2+}$	27	2.8
$\text{D2}_2\text{B}^{2+}$	18	2.9
$\text{D3}_2\text{B}^{2+}$	9.3	2.3

within both (symmetric and nonsymmetric) dendrimer families. Therefore, in low-polarity solvent the dendritic branches disfavor, to some extent, the recognition of the 4,4'-bipyridinium core by the receptor. In  $\text{CH}_2\text{Cl}_2/\text{CH}_3\text{CN}$  1:3 (v/v) solution the association constants are 1 order of magnitude lower and quite similar for all the investigated dendrimers (Table 2). This trend has also been observed by performing  $^1\text{H}$  NMR measurements in pure  $\text{CD}_2\text{Cl}_2$  and  $\text{CD}_2\text{Cl}_2/\text{acetone-}d_6$  1:2 (v/v) or  $\text{CDCl}_3/\text{acetone-}d_6$  1:2 (v/v).<sup>5</sup>

The results of these investigations show that by increasing the polarity of the medium the stability of the complexes decreases and loses its dependence by the number and the generation of the dendrons appended to the 4,4'-bipyridinium core. Such experimental evidence is in agreement with the expectation because in a more polar solvent the electron donor–acceptor interactions are weaker, i.e., solvation of the hydrophilic dicationic core by higher polarity solvent molecules competes with “solvation” of the core by the host cavity more efficiently than in lower polarity solvent.

Ion pairing should be taken into account when adduct formation involves charged species and occurs in low dielectric media. In particular, if the formation of inclusion complexes involves previous ion-pair dissociation, the apparent

stability constants are known to be concentration dependent.<sup>22</sup> In the present case, however, similar binding constant values have been obtained by independent titration experiments performed in air-equilibrated  $\text{CH}_2\text{Cl}_2$  or  $\text{CD}_2\text{Cl}_2$  solutions at 298 K and with concentration values that range between  $10^{-5}$  to  $10^{-4}$  M and  $5 \times 10^{-4}$  to  $5 \times 10^{-3}$  M by using the spectrofluorimetric technique and  $^1\text{H}$  NMR measurements, respectively.<sup>5</sup> It follows that complex formation does not require ion-pair dissociation and ion-paired adducts are formed:



Nevertheless, to simplify the representation of the dendrimers, the model compound, and their supramolecular adducts,  $\text{PF}_6^-$  counteranions have always been omitted.

To compare the results obtained by fluorescence and electrochemical experiments, the effect of  $\text{NBu}_4\text{PF}_6$  addition on the stability of the host–guest complexes in  $\text{CH}_2\text{Cl}_2$  solution have also been investigated. In particular, the behavior of  $\text{D1}_2\text{B}^{2+}$ ,  $\text{D3B}^{2+}$ , and  $\text{D3}_2\text{B}^{2+}$  dendrimers and  $\text{doB}^{2+}$  model compound have been examined in order to investigate the effect of the number and generation of the appended dendrons.

Upon addition of  $\text{NBu}_4\text{PF}_6$  (up to 0.14 M) to a  $\text{CH}_2\text{Cl}_2$  solution of **T**, absorption and emission spectra of **T** do not show any appreciable change (compare spectra represented by black and gray solid lines in Figure 5), so that no competition of  $\text{Bu}_4\text{N}^+$  for the **T** hosting cavity is expected. No significant change in the absorption spectrum of a  $\text{CH}_2\text{Cl}_2$  solution of  $\text{D}_3\text{B}^{2+}$  has also been observed upon addition of  $\text{NBu}_4\text{PF}_6$  (up to 0.14 M). On the other hand, titration of a  $\text{CH}_2\text{Cl}_2$  solution of **T** containing 0.14 M  $\text{NBu}_4\text{PF}_6$  with  $\text{D}_3\text{B}^{2+}$  shows a stronger decrease of fluorescence compared to the same titration performed in the absence of salt (compare the spectra represented by dashed black and gray lines in Figure 5). The association constant raises from  $9300 \text{ M}^{-1}$  when no salt is present in solution to  $23000 \text{ M}^{-1}$  at  $[\text{NBu}_4\text{PF}_6] = 0.14 \text{ M}$ .

Qualitatively similar results have been obtained by titrating with  $\text{D}_3\text{B}^{2+}$  dendrimer  $\text{CH}_2\text{Cl}_2$  solutions of **T** containing  $\text{NET}_4\text{PF}_6$ ,  $\text{NET}_4\text{BF}_4$ ,  $\text{NBu}_4\text{BF}_4$ , and  $\text{NBu}_4\text{BPh}_4$  salts.

Spectrofluorimetric titrations of  $\text{CH}_2\text{Cl}_2$  air-equilibrated solutions of ca.  $10 \mu\text{M}$  **T** at different  $\text{NBu}_4\text{PF}_6$  concentrations with  $\text{D1}_2\text{B}^{2+}$ ,  $\text{D3B}^{2+}$ , and  $\text{D3}_2\text{B}^{2+}$  dendrimers and model compound  $\text{doB}^{2+}$  evidence that salt addition affects the thermodynamic stability of the host–guest complexes. In particular, the ratio  $K_{\text{ass}}/K_{\text{ass}}^0$ , where  $K_{\text{ass}}$  and  $K_{\text{ass}}^0$  are the value of association constants obtained in the presence and absence of salt (Figure 6), respectively, shows that (i) for model compound  $\text{doB}^{2+}$  the effect is small and quantitatively equal upon addition of 1 or 100 mM  $\text{NBu}_4\text{PF}_6$ , (ii) for the investigated dendrimers, upon addition of a high concentration of salt (100 mM) ca. 2.5-fold increase in  $K_{\text{ass}}$  is observed, but (iii) at low salt concentration (1 mM), the behavior of the three dendrimers is different and  $K_{\text{ass}}$  is practically unaffected only in the case of  $\text{D3}_2\text{B}^{2+}$ .

(22) Huang, F.; Jones, J.; Slebodnick, C.; Gibson, H. W. *J. Am. Chem. Soc.* **2003**, *125*, 14458.

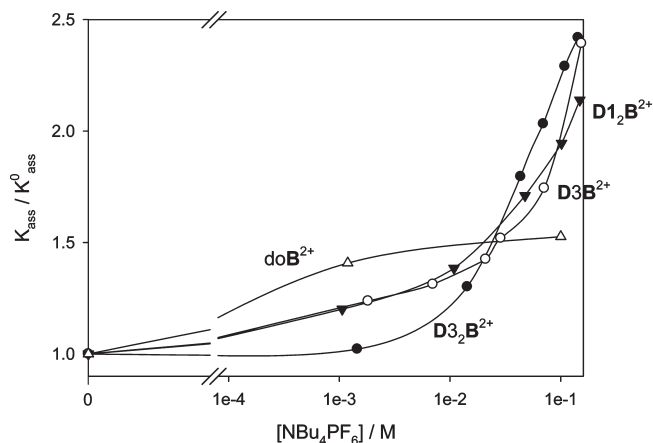


**FIGURE 6.** Plot of the association constant ratio obtained in the absence ( $K_{\text{ass}}^0$ ) and in the presence of increasing amounts ( $K_{\text{ass}}$ ) of  $\text{NBu}_4\text{PF}_6$ , for  $\text{D}_3\text{B}^{2+}$  (solid circles),  $\text{D}_3\text{B}^{2+}$  (open circles),  $\text{D}_{12}\text{B}^{2+}$  (solid triangles), and  $\text{doB}^{2+}$  (open triangles) in air-equilibrated  $\text{CH}_2\text{Cl}_2$  solution at 298 K.

The observed effect on association constants cannot be attributed to counterion assisted complexation<sup>23</sup> or allosteric effects.<sup>24</sup> Indeed, a large excess of salt is needed (at least 100-fold excess) to see a sizable change in the association constants of dendrimers with **T**. Moreover, as previously discussed, under the investigated conditions, the bipyridinium core is always ion-paired to its  $\text{PF}_6^-$  counterions. Therefore, the trend reported in Figure 6 cannot be ascribed to a change in the medium properties: because  $\text{NBu}_4^+$  and  $\text{PF}_6^-$  ions are almost completely associated in  $\text{CH}_2\text{Cl}_2$  solution, the Debye–Hückel model is not suitable to describe the present effect. An explanation can be obtained from the NMR experiments which show that the addition of  $\text{NBu}_4\text{PF}_6$  to  $\text{CH}_2\text{Cl}_2$  dendrimer solutions causes a change in dendrimer conformation consistent with dendron unfolding. Therefore, the observed increase in the association constants demonstrates that dendron unfolding stabilizes the host–guest complex between **T** and dendrimers. The results also show that the salt concentration required to induce a significant effect on the association constant increases by increasing dendron generation. On the other hand, the modest effect observed for the model compound  $\text{doB}^{2+}$  can be attributed to the presence of alkyl chains instead of polyaryl-ether dendrons.

Summarizing, an increase in solvent polarity (upon addition of  $\text{CH}_3\text{CN}$  to  $\text{CH}_2\text{Cl}_2$ ) leads to a strong decrease of the association constants (more than 1 order of magnitude), while addition of  $\text{NBu}_4\text{PF}_6$  up to 0.15 M brings about an increase (ca. 2.5 fold) in association constants. These apparently contrasting behaviors can be rationalized considering that in the first case a significant increase of polarity causes a lowering of electron donor–acceptor interactions since both the host and the guest are efficiently stabilized by the solvent. In the latter case, the solvent polarity is only slightly affected by the presence of  $\text{NBu}_4\text{PF}_6$ , which is far from being completely dissociated in  $\text{CH}_2\text{Cl}_2$  solution, and therefore the observed effect is ascribed to a dendron un-

**TABLE 3.** Rate Constants for the Formation ( $k_f$ ) and Dissociation ( $k_b$ ) of the Host–Guest Complex between Tweezer **T** and  $\text{Dn}_m\text{B}^{2+}$  Dendrimers in Air-Equilibrated  $\text{CH}_2\text{Cl}_2$  Solution at 293 K

$\text{T} \cdot \text{Dn}_m\text{B}^{2+}$	$k_f / \text{M}^{-1} \text{s}^{-1}$	$k_b / \text{s}^{-1}$
$\text{D1B}^{2+}$	$\geq 10^8$	$\geq 10^3$
$\text{D2B}^{2+}$	$\geq 10^8$	$\geq 10^3$
$\text{D3B}^{2+}$	$\geq 10^8$	$\geq 10^3$
$\text{D}_{12}\text{B}^{2+}$	$1.9 \times 10^7$	700
$\text{D}_{22}\text{B}^{2+}$	$7.7 \times 10^6$	430
$\text{D}_{32}\text{B}^{2+}$	$2.8 \times 10^6$	300

folding process that opens the dendrimer structure so that the resulting host–guest complex is more stable.

**Kinetic of Complex Formation: Stopped-Flow Measurements.** Measurements of fluorescence intensity of **T** upon addition of dendrimers in a stopped-flow apparatus enabled information to be gained on the kinetics of host–guest complex formation. The fluorescence intensity at  $\lambda > 335$  nm arises from the uncomplexed host molecules and the fitting of the data obtained during the titrations (see the Experimental Section) shows that upon addition of dendrimers of the same generation the decay of the **T** fluorescence is slower in the case of the symmetric than for nonsymmetric ones (Table 3). This finding can be accounted for by the two different mechanisms of complexation evidenced by NMR measurements:<sup>5b</sup> clipping for symmetric dendrimers and threading for nonsymmetric ones. Moreover, within symmetric  $\text{Dn}_2\text{B}^{2+}$  dendrimers the clipping process is slower as dendrimer generation increases (Table 3), as expected because of the increased steric hindrance of the appended dendrons that have to rearrange their conformation in order to enable the binding of the dendritic core.

The effect of  $\text{NBu}_4\text{PF}_6$  addition on the kinetics of the complex formation between **T** and  $\text{D}_3\text{B}^{2+}$  dendrimer has also been investigated in an air-equilibrated  $\text{CH}_2\text{Cl}_2$  solution of 14  $\mu\text{M}$  **T** containing 1 equiv of dendrimer at 293 K. The rate of **T** fluorescence decay decreases by increasing the salt content (compare the decays represented by gray squares and black circles in Figure 7). Lower complex formation and

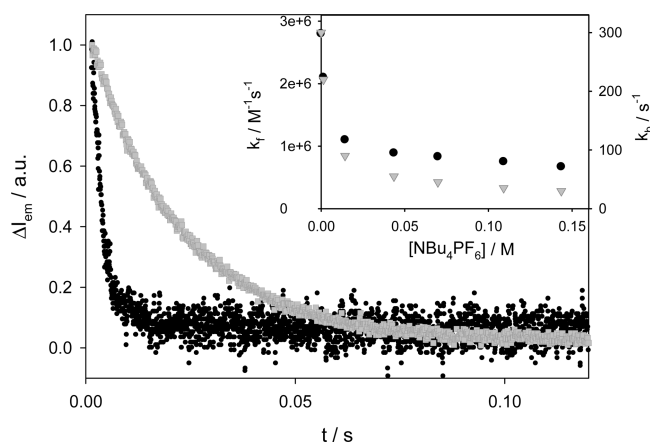


**FIGURE 7.** Fluorescence decay of 14  $\mu\text{M}$  **T** air-equilibrated  $\text{CH}_2\text{Cl}_2$  solution at 293 K containing 1 equiv of  $\text{D}_3\text{B}^{2+}$  in the absence (black circles) and presence of 0.14 M  $\text{NBu}_4\text{PF}_6$  (gray squares);  $\lambda_{\text{ex}} = 297$  nm. The inset shows the kinetics constants for association ( $k_f$ , black circles) and dissociation ( $k_b$ , gray triangles) processes between **T** and  $\text{D}_3\text{B}^{2+}$  plotted versus  $\text{NBu}_4\text{PF}_6$  concentration.

(23) A few equivalents of salt does not influence complex formation. For references on this topic see: Jones, J. W.; Zakharov, L. N.; Rheingold, A. L.; Gibson, H. W. *J. Am. Chem. Soc.* **2002**, *124*, 13378.

(24) (a) Arduini, A.; Giorgi, G.; Pochini, A.; Secchi, A.; Uguzzoli, F. *J. Org. Chem.* **2001**, *66*, 8302. (b) Kubik, S. *J. Am. Chem. Soc.* **1999**, *121*, 5846.

**TABLE 4.** Rate Constants for the Formation ( $k_f$ ) and Dissociation ( $k_b$ ) of the Host–Guest Complex between Tweezer **T** and  $D_3B^{2+}$  Dendrimer in Air-Equilibrated  $CH_2Cl_2$  Solution at 293 K at Different Concentrations of  $NBu_4PF_6$

$[NBu_4PF_6]/M$	$k_f/M^{-1} s^{-1}$	$k_b/s^{-1}$
0	$2.8 \times 10^6$	300
$1.5 \times 10^{-3}$	$2.1 \times 10^6$	220
$1.4 \times 10^{-2}$	$1.1 \times 10^6$	90
$4.4 \times 10^{-2}$	$8.9 \times 10^5$	55
$7.0 \times 10^{-2}$	$8.3 \times 10^5$	45
$1.1 \times 10^{-1}$	$7.5 \times 10^5$	35
$1.4 \times 10^{-1}$	$6.7 \times 10^5$	30

dissociation rate constants are obtained upon increasing  $NBu_4PF_6$  concentration (Table 4).

This behavior is consistent with the lower diffusion coefficients of the dendrimers obtained from the NMR techniques. A closer inspection to Figures 3 and 7 shows that the diffusion coefficients of dendrimers decrease linearly with  $NBu_4PF_6$  concentration, while the rate constants  $k_f$  and  $k_b$  show a stronger dependence on salt concentration. This points to a quite complex kinetic behavior: dendron folding/unfolding processes affect not only the diffusion coefficient of the dendrimers but also the kinetics of formation/dissociation of the host–guest complex.

## Conclusions

Host–guest complex formation between a molecular tweezer **T** and 4,4'-bipyridinium cored dendrimers  $D_nB^{2+}$  has been investigated by NMR, absorption, and emission spectroscopy, as well as electrochemical measurements. The complex formation is mainly driven by electron donor/acceptor interactions. The effect of solvent polarity and addition of  $NBu_4PF_6$  on both the thermodynamic and kinetic features of the association process have been investigated.

As to the *thermodynamic properties*, in  $CH_2Cl_2$  association constant values (i) are higher for nonsymmetric  $D_nB^{2+}$  dendrimers than for the corresponding symmetric  $D_nB^{2+}$  ones, (ii) within each dendrimer family, they decrease by increasing generation of the dendrons, and (iii) they increase (by ca. 2.5 fold) upon addition of  $NBu_4PF_6$  (0.15 M). In higher polarity mixtures, such as  $CH_2Cl_2/CH_3CN$  1:3 (v/v), association constants are one order of magnitude lower and almost unaffected by dendrimer generation and symmetry. These experimental results can be interpreted as follows: (a) an increase of solvent polarity (by addition of  $CH_3CN$ ) leads to a better stabilization of the host and guest species by solvent molecules, thus disfavoring charge-transfer interactions between dendrimers and tweezer and (b) addition of  $NBu_4PF_6$  to the solutions in low-polar solvents causes a change in dendrimer conformation that can be ascribed to dendron unfolding. The unfolded structure stabilizes the host–guest complex, as demonstrated by the increase in the association constants.

The *kinetic features* of complex formation and dissociation show that in a polar solvent the rate constants are higher for the nonsymmetric  $D_nB^{2+}$  dendrimers compared to those for the symmetric  $D_nB^{2+}$  ones, and decrease by increasing

dendrimer generation within the symmetric family, and by adding  $NBu_4PF_6$ , as a result of dendron unfolding.

The present work demonstrates the importance of taking into account the effects exerted by salt addition when both spectroscopic and electrochemical techniques are exploited to characterize electron donor/acceptor complexes in low polarity solvents, especially when charged species are involved. In such cases, the addition of supporting electrolytes required in electrochemical experiments might modify the dendrimer conformation inducing unfolding of the branches, a behavior that strengthens analogies between dendrimers and proteins.<sup>25</sup> These conformational changes should be considered when designing dendrimers for drug delivery and catalysis purposes or sensing applications.

## Experimental Section

**Materials.** Nonsymmetric and symmetric dendrimers<sup>13</sup> and receptor **T**<sup>4a</sup> have been synthesized according to previously published procedures. 1,1'-Dioctyl-4,4'-bipyridinium has been kindly provided by Prof. Arduini.  $NBu_4PF_6$  has been purchased by Fluka and used after being dried in an oven at 70 °C and then by vacuum.

**Photophysical Measurements.** Absorption and emission spectra, emission quantum yields, excited state lifetimes, and transient absorption spectra were measured in air-equilibrated solutions of  $CH_2Cl_2$  and  $CH_3CN$  (Merck UVASOL) at 298 K. Absorption spectra were recorded by a Perkin-Elmer  $\lambda$ 40 spectrophotometer while emission spectra were recorded on a Perkin-Elmer LS50 spectrofluorimeter. In the titration experiments, excitation was performed at the lower excited state of the **T** molecule. Fluorescence lifetimes were measured by an Edinburgh FLS920 spectrofluorimeter. The excitation pulse at 334 nm is obtained by a gas discharge lamp (model nF900, filled with deuterium) delivering pulses of 0.5 ns at fwhm working at a frequency of 40 kHz. A photomultiplier tube (Hamamatsu R928P) cooled at 253 K and suitably amplified is used as a stop detector. A TCC900 card for data acquisition is used. Implemented software enabled deconvolution of the excitation profile by the radiative decay profile. Transient absorption spectra were determined in deaerated solutions obtained by consecutive freeze–pump–thaw cycles by means of a Continuum Surelite SLI-10 Nd:YAG laser that has been used to excite the sample through its fourth harmonic generating 10-ns pulses at 266 nm at a frequency of 1 kHz. The monitoring beam is supplied by a Xe arc lamp, and the signal detected by a red sensitive photodiode after passing through a high radiance monochromator, then recorded by a Tektronix TDS640A digitizer oscilloscope and transferred to a PC computer. Differential absorption spectra are recorded point-by-point at a fixed wavelength, where also kinetic measurements were made. Thirty two individual laser shots have been averaged to improve the reliability of each acquisition. The estimated experimental errors are  $\pm 2$  nm on the band maximum,  $\pm 5\%$  on the molar absorption coefficient and excited state lifetimes, and  $\pm 10\%$  on the emission quantum yield.

**Association Constants by Fluorescence Measurements.** Given the equilibrium reaction between the host (H) and the added guest (G) leading to the adduct (HG):



(25) (a) Beringhelli, T.; Eberini, I.; Galliano, M.; Pedoto, A.; Perduca, M.; Sportiello, A.; Fontana, E.; Monaco, H. L.; Gianazza, E. *Biochemistry* **2002**, *41*, 15415. (b) Jelesarov, I.; Eberhard, D.; Thomas, R. M.; Bosshard, H. R. *Biochemistry* **1998**, *37*, 7539.



the association constant of the inclusion complex formation is

$$K_{\text{ass}} = \frac{[\text{HG}]_{\text{eq}}}{[\text{H}]_{\text{eq}}[\text{G}]_{\text{eq}}} = \frac{[\text{HG}]_{\text{eq}}}{([\text{H}]_0 - [\text{HG}]_{\text{eq}})([\text{G}]_0 - [\text{HG}]_{\text{eq}})} \quad (6)$$

The observed luminescence intensity arising from excited free host molecules, after being corrected for geometrical factor and inner filter effects,<sup>26</sup> is related to the equilibrium concentration of the inclusion complex  $[\text{HG}]_{\text{eq}}$  formed in solution,

$$I_{\text{obs}} = I_{\text{H}}[\text{H}]_0 + (I_{\text{HG}} - I_{\text{H}})[\text{HG}]_{\text{eq}} + I_{\text{G}}([\text{G}]_0 - [\text{HG}]_{\text{eq}}) \quad (7)$$

where  $I_{\text{H}}$  represents a parameter linearly proportional to the fluorescence quantum yield of the host,  $I_{\text{HG}} = 0$  as revealed by fluorescence lifetime measurements, and  $I_{\text{G}}$  is negligible for all the dendrimers, while model compound  $\text{doB}^{2+}$  as the  $\text{PF}_6^-$  salt exhibits fluorescence.<sup>5b,27</sup>  $[\text{HG}]_{\text{eq}}$  can be derived by eq 2:

$$[\text{HG}]_{\text{eq}} = \frac{1}{2K_{\text{ass}}} (a - \sqrt{a^2 - 4K_{\text{ass}}^2[\text{H}]_0[\text{G}]_0}) \quad (8)$$

where  $a = (K_{\text{ass}}[\text{H}]_0 + K_{\text{ass}}[\text{G}]_0 + 1)$

**Stopped-Flow Experiments.** The experiments were performed in air-equilibrated  $\text{CH}_2\text{Cl}_2$  solutions of **T** and equimolar  $\text{CH}_2\text{Cl}_2/\text{CH}_3\text{CN}$  9:1 (v/v) solutions of  $\text{Dn}_m\text{B}^{2+}$  with Applied Photophysics SX 18-MV equipment. The standard flow tube has an observation path length of 1.0 cm, and the driving ram for the mixing system was operated at the recommended pressure of 8.5 bar. Under these conditions the time required to fill the cell was 1.35 ms. A baseline correction was applied to take into account the dependence of the instrument response on pressure. The reactions were monitored by the decrease of the emission at  $\lambda > 335$  nm with  $\lambda_{\text{ex}} = 297$  nm. In all the experiments, the cell block and drive syringes were thermostated by using a circulating constant-temperature bath maintained at the required temperature.

Rate constants for the complex formation between the host **T** and dendritic  $\text{Dn}_m\text{B}^{2+}$  guests have been determined, taking into account the equilibrium between the reagents H and G and the product HG as already expressed in eq 1:

$$-\frac{d[\text{H}]}{dt} = \frac{d[\text{HG}]}{dt} = k_{\text{f}}[\text{H}][\text{G}] - k_{\text{b}}[\text{HG}] \quad (9)$$

where the forward ( $k_{\text{f}}$ ) and backward ( $k_{\text{b}}$ ) kinetic constants are related by:

$$K_{\text{ass}} = \frac{k_{\text{f}}}{k_{\text{b}}} \quad (10)$$

The observed fluorescence intensity at  $\lambda > 335$  nm arises from the uncomplexed host molecules and is related to the concentration of the supramolecular adduct  $[\text{HG}]$  by eq 7:

$$I_{\text{obs}} = I_{\text{H}}[\text{H}] = I_{\text{H}}([\text{H}]_0 - [\text{HG}]) \quad (11)$$

where  $I_{\text{H}}$  represents a parameter linearly proportional to the fluorescence quantum yield of the host and  $[\text{HG}]$  can be derived by eq 8 considering that  $[\text{H}] = [\text{G}]$ :

$$[\text{HG}]_i = \frac{(p-q)(e^{qt} - 1)}{2k_{\text{f}} \left(1 - \frac{p-q}{p+q} e^{qt}\right)} \quad (12)$$

where  $p = -k_{\text{b}} - 2k_{\text{f}}[\text{H}]_0$  and  $q = \{k_{\text{b}}^2 + 4k_{\text{f}}k_{\text{b}}[\text{H}]_0\}^{1/2}$ .

**Electrochemical Experiments.** All electrochemical measurements were carried out in argon-purged  $\text{CH}_2\text{Cl}_2/\text{CH}_3\text{CN}$  9:1 (v/v) solutions (Romil Hi-Dry) at room temperature with an Autolab 30 multipurpose instrument interfaced to a personal computer. In cyclic voltammetric experiments the working electrode was a glassy carbon electrode (0.08  $\text{cm}^2$ , Amel); its surface was routinely polished with 0.3 mm alumina–water slurry on a felt surface, immediately prior to use. In all cases, the counter electrode was a Pt spiral, separated from the bulk solution with a fine glass frit, and an Ag wire was used as a quasireference electrode. Ferrocene ( $E_{1/2} = +0.46$  V vs. SCE) was present as an internal standard. In all the electrochemical experiments the concentration of the compounds was in the range  $5 \times 10^{-4}$  to  $1 \times 10^{-3}$  M, and 0.1 M tetrabutylammonium hexafluorophosphate was added as the supporting electrolyte. Cyclic voltammograms were obtained with sweep rates in the range 0.02–1.0  $\text{V s}^{-1}$ ; the IR compensation implemented within the Autolab 30 was used, and every effort was made throughout the experiments in order to minimize the resistance of the solution. In any instance, the full reversibility of the voltammetric wave of ferrocene was taken as an indicator of the absence of uncompensated resistance effects. The reversibility of the observed processes was established by using the criteria of (1) separation of 60 mV between cathodic and anodic peaks, (2) the close to unity ratio of the intensities of the cathodic and anodic currents, and (3) the constancy of the peak potential on changing sweep rate in the cyclic voltammograms. The experimental error on the potential values was estimated to be 10 mV. The diffusion coefficients and the numbers of exchanged electrons were obtained independently by chronoamperometry as described in the literature.<sup>29</sup> A Pt disk with a diameter of 50  $\mu\text{m}$  was used as a working electrode and the experiments were carried out for 5 s, with 0.05 s sample time, at the potential values of  $-0.35$  V for  $\text{D}_2\text{B}^{2+}$ . The current intensities in steady-state conditions were determined from CV experiments by using the same working electrode of the chronoamperometric experiments and sweep rate of 10  $\text{mV s}^{-1}$ .

**NMR Measurements.**  $^1\text{H}$  NMR spectra at 295 K were obtained at 600 MHz in  $\text{CD}_2\text{Cl}_2/\text{CD}_3\text{CN}$  9:1 (v/v) and  $\text{CD}_3\text{CN}$  on a Varian Inova spectrometer. DOSY experiments were recorded with the same apparatus equipped with a PFG triple-resonance inverse detection probe, by means of the BPLED pulse sequence.<sup>28</sup> Delay diffusion was 0.020 or 0.025 s. Gradient strength was varied from 0.4 to 66 G/cm. Gradient calibration was obtained on a HDO/ $\text{D}_2\text{O}$  sample, for which the diffusion coefficient was known<sup>29</sup> ( $19.2 \times 10^{-10} \text{ m}^2 \text{ s}^{-1}$ ). The diffusion coefficient  $D$  was obtained from the Stejskal–Tanner equation,<sup>28</sup> and the hydrodynamic radius was evaluated by the Stokes–Einstein equation. The viscosity of the medium was measured by an Ubbelohde viscosimeter and the experimental error is  $\pm 0.0001 \text{ mPa}\cdot\text{s}$ .

**Acknowledgment.** The authors would like to thank Dr. Francesco Scagnolari and Dr. Stefano Ottani for viscosity measurements and Prof. Vincenzo Balzani for useful discussions. This work has been supported in Italy by Fondazione Carisbo (“Dispositivi nanometrici basati su dendrimeri e nanoparticelle”).

(26) Credi, A.; Prodi, L. *Spectrochim. Acta, Part A* **1998**, *54*, 159.

(27) (a) Peon, J.; Tan, X.; Hoerner, D.; Xia, C.; Luk, Y. F.; Kohler, B. *J. Phys. Chem. A* **2001**, *105*, 5768. (b) Credi, A.; Dumas, S.; Silvi, S.; Venturi, M.; Arduini, A.; Pochini, A.; Secchi, A. *J. Org. Chem.* **2004**, *69*, 5881.

(28) Wu, D.; Chen, A.; Johnson, C. S., Jr. *J. Magn. Reson. A* **1995**, *115*, 260.

(29) Tyrrell, H. J. W.; Harris, K. R. *Diffusion in Liquids*; Butter-Worth: London, UK, 1984.